Available online at www.sciencedirect.com
ScienceDirect
Journal of Sound and Vibration 314 (2008) 481–506
JOURNAL OF SOUND AND VIBRATION
www.elsevier.com/locate/jsvi

Cluster vector-based control of a flexible beam for generating a vibration-free region

Nobuo Tanaka*, Hiroyuki Iwamoto

Department of Aerospace Engineering, Tokyo Metropolitan University, 6-6 Asahigaoka, Hino-city, Tokyo 191-0065, Japan

Received 6 February 2007; received in revised form 10 September 2007; accepted 31 December 2007
Handling Editor: J. Lam
Available online 7 March 2008

Abstract

This paper presents cluster vector-based control for generating a vibration-free state in the designated area of a target beam. Cluster control consisting of both cluster filtering and cluster actuation is shown, and the stability of a cluster control system is investigated. Cluster filtering aims at extracting the information necessary for control, while cluster actuation excites or suppresses the cluster filtering output without causing spillover. For generating a vibration-free state in the designated area of a beam, where neither progressive waves nor reflected waves exist, state variables governing the vibration of a beam must be extracted and suppressed. A cluster vector—the common link between cluster filtering and cluster actuation—is introduced for this purpose. It is found that the suppression of a performance index, expressed in terms of the cluster vector, generates a vibration-free state of a beam, whereas the suppression of conventional orthogonal contributors, such as radiation modes, does not. Numerical simulation is performed, followed by an experiment, to verify the validity of the results.
© 2008 Elsevier Ltd. All rights reserved.

1. Introduction

When suppressing the vibration of a distributed-parameter structure, control designers face the problem of its infinite number of vibration modes. Of all the vibration control methodologies reported so far, there exist two control strategies that can deal with an infinite number of structural modes. Direct velocity feedback (DVFB) [1,2] is one such method, which uses collocated velocity sensors and actuators, enabling the augmentation of the damping of all structural modes. However, this method is considered a low-authority control (LAC) [3], because it is not capable of controlling specific modes of interest. The other control strategy is active wave-absorbing control [4–12], which is based on the excitation mechanism of structural modes. By suppressing the reflected waves induced in a structure, active wave-absorbing control inactivates all structural modes, rather than augmenting the damping of a structure. Thus, active wave-absorbing control may be considered as a process of implanting the characteristics of an infinite structure, wherein no vibration modes occur, onto a finite structure.

*Corresponding author. Tel./fax: +81 42 585 8668.
E-mail address: ntanaka@cc.tmit.ac.jp (N. Tanaka).

0022-460X/$ - see front matter © 2008 Elsevier Ltd. All rights reserved.
doi:10.1016/j.jsv.2007.12.042

Nomenclature

A	cross-sectional area
$\mathbf{A}$	error weighting matrix
E	Young's modulus
$f_i(t)$	control force at ith point
$f_{di}(t)$	disturbance force at ith point
$\mathbf{f}$	control force vector
$\tilde{\mathbf{f}}$	cluster control force vector
$\hat{\mathbf{f}}$	transformed force vector
$\mathbf{G}$	gain matrix
I	second moment of area
J	performance index
l_0	beam length
$\mathbf{L}$	transformation matrix
$m_x(x)$	beam bending moment
N_d	number of point disturbance forces
N_m	number of point control forces
N_s	number of velocity sensors
$\mathbf{P}$	nonsingular matrix
$q_x(x)$	beam shear force
$\mathbf{Q}$	orthonormal transformation matrix
$^{\mathrm{T}}$	transpose of expression
$\mathbf{T}$	nonsingular matrix
$\mathbf{T}_0$	nonsingular transformation matrix
$\mathbf{T}_{ij}$	transfer matrix between nodes i and j
$\mathbf{u}$	radiation mode vector
$\mathbf{z}_i$	ith state vector
δ_{rs}	Kronecker's delta function
$\delta(x)$	Dirac's delta function
Δ	sensing interval
$\eta_k(t)$	kth modal coefficient
$\boldsymbol{\eta}$	modal amplitude vector
$\theta(x)$	beam slope
$\mathbf{\Lambda}_G$	diagonal gain matrix
$\xi(x, t)$	beam deflection
$\boldsymbol{\xi}$	displacement vector
$\hat{\boldsymbol{\xi}}$	transformed vector
$\tilde{\boldsymbol{\xi}}$	cluster vector
ρ	mass density
$\varphi_k(x)$	kth eigenfunction
$\boldsymbol{\varphi}$	eigenfunction vector
$\boldsymbol{\psi}$	power mode eigenfunctions
ω_r	rth resonance frequency
$\mathbf{\Omega}_\omega$	transfer function matrix between control force and displacement vectors
$\dot{\xi}$	time derivative of ξ

It is possible to group all the structural modes into a finite number of clusters [13], wherein all the structural modes belonging to a particular cluster have the same common attributes. If the structural modes within a given cluster are orthogonal to those in other clusters, the clusters may be controlled independently, thereby enabling cluster control using a simple control strategy without causing spillover problems. Grouping all the structural modes into a finite number of clusters is called cluster filtering [13], while independent control of each cluster is termed cluster actuation [13]. Utilizing both cluster filtering and cluster actuation, cluster control [13–15] may be performed. This approach is categorized as middle-authority control (MAC) [13], whose characteristics lie between those of conventional LAC and high-authority control (HAC). Cluster control offers the benefits of stability and control law simplicity analogous to LAC, while providing the high control performance and some flexibility of control gain assignment of HAC.

Vibration control has long been considered as a control technique for augmenting the damping of structural modes. However, even after perfectly augmenting the damping of structural modes, vibrations still occur in the structure. Note that a perfect control performance over the frequency response of a structure, with dynamic compliance, dynamic mobility, etc., results in convergence to the asymptote of the frequency response. Thus, a conventional control approach, even when ideally performed, may not produce a vibration-free state.

Currently, there is a strong demand for vibration-free structures, particularly in the field of nanotechnology. A recently disclosed technology road map, outlining a future generation of semiconductor technology, shows that a 22-nm-wide (i.e. only 100 atoms wide) electrical lead wire is planned as a technological milestone. However, no existing technology can cope with this demand. Realizing future semiconductors, with highly sophisticated specifications, requires the resolution of many technological implementation problems. Among them, the establishment of a nano-infrastructure, which requires semiconductor fabrication machines with extremely low vibration levels, is essential.

Instead of further enhancing structural damping, which is the aim of traditional vibration control, a novel vibration control approach that can even eliminate micro-vibration is needed to keep pace with the demands

for continually increased precision. Moreover, the final goal of vibration control is straightforward—the new method should generate a vibration-free state of the target structure.

By expanding on the concept of active cluster control [13–15], this paper presents a novel control strategy that enables the creation of a stable, vibration-free state in the designated region of a flexible beam. This paper begins by discussing the cluster control system of a distributed-parameter beam for generating a vibration-free state in the designated area of a target beam. Next, cluster control consisting of both cluster filtering and cluster actuation is shown, and an investigation of the stability of a cluster control system is presented. Cluster filtering extracts the information necessary for control, while cluster actuation excites or suppresses the cluster filtering output without causing spillover. For generating a vibration-free state in the designated area of a beam, state variables governing beam vibration must be extracted and suppressed. For this purpose, a cluster vector that serves as the common link between cluster filtering and cluster actuation is introduced. Furthermore, a means of establishing the cluster vector is presented and its properties are clarified. It is found that the suppression of a performance index, expressed in terms of the cluster vector, leads to the generation of a vibration-free state, whereas the suppression of conventional orthogonal contributors, such as radiation modes (sometimes termed power modes), does not. Finally, numerical simulation and experiments verify the validity of the cluster control presented in the work.

2. Cluster control of a beam, general description

This paper deals with a Euler–Bernoulli beam with any boundary condition at both ends of the beam with N_m point control forces $f_i(t)$ and N_d point disturbance forces $f_{d,i}(t)$ acting at x_i $(i = 1\sim N_m)$ and $x_{d,i}$ $(i = 1\sim N_d)$, respectively. The equation of motion of a beam is then given by

$$EI\frac{\partial^4\xi(x,t)}{\partial x^4}+\rho A\frac{\partial^2\xi(x,t)}{\partial t^2}=\sum_{i=1}^{N_m}f_i(t)\delta(x-x_i)+\sum_{i=1}^{N_m}f_{d,i}(t)\delta(x-x_{d,i})$$
$$=\mathbf{f}^{\mathrm{T}}(t)\boldsymbol{\delta}+\mathbf{f}_d^{\mathrm{T}}(t)\boldsymbol{\delta}_d, \tag{1}$$

where

$$\mathbf{f}^{\mathrm{T}}(t)=\begin{pmatrix} f_1(t) & f_2(t) & \cdots & f_{N_m}(t)\end{pmatrix}, \tag{2}$$

$$\boldsymbol{\delta}^{\mathrm{T}}=(\delta(x-x_1)\quad \delta(x-x_2)\quad \cdots\quad \delta(x-x_{N_m})), \tag{3}$$

$$\boldsymbol{\delta}_d^{\mathrm{T}}=\mathrm{col}(\delta(x-x_{d,1})\quad \delta(x-x_{d,2})\quad \cdots\quad \delta(x-x_{d,N_d})) \tag{4}$$

and where $\xi(x,t)$, E, I, ρ, A, t, δ and T denote the flexural deflection of a beam at x, Young's modulus, the second moment of area, mass density, cross-sectional area, time, the delta function and transpose of the expression, respectively. Using the eigenfunction $\varphi_k(x)$ and the associated modal coefficient $\eta_k(t)$ of a beam, the beam deflection $\xi(x,t)$ is written as

$$\xi(x,t)=\sum_{k=1}^{\infty}\varphi_k(x)\eta_k(t). \tag{5}$$

Assume that the eigenfunctions are orthogonal and normalized as

$$\int_0^{l_0}EI\varphi_r(x)\frac{\mathrm{d}^4\varphi_s}{\mathrm{d}x^4}\,\mathrm{d}x=\omega_r^2\delta_{rs}, \tag{6}$$

$$\int_0^{l_0}\rho A\varphi_r(x)\varphi_s(x)\mathrm{d}x=\delta_{rs}, \tag{7}$$

where l_0 is the beam length, ω_r is the rth resonance frequency and δ_{rs} is the Kronecker's delta function. Then, the modal coefficient $\eta_k(t)$ is expressed as

$$\eta_k(t)=\int_0^{l_0}\varphi_k(x)\xi(x,t)\mathrm{d}x. \tag{8}$$

Multiplying $\varphi_s(x)$ on both sides of Eq. (1), integrating it over the domain of the target beam and substituting Eqs. (6) and (7) into Eq. (1) produce an equation of motion in a modal coordinate system,

$$\ddot{\eta}_s(t) + \omega_s^2 \eta_s(t) = \mathbf{f}^{\mathrm{T}}(t)\boldsymbol{\varphi}_s + \mathbf{f}_d^{\mathrm{T}}(t)\boldsymbol{\varphi}_{s,d} \quad (s = 1, 2, 3, \ldots), \tag{9}$$

where

$$\boldsymbol{\varphi}_s = \begin{pmatrix} \varphi_s(x_1) \\ \varphi_s(x_2) \\ \vdots \\ \varphi_s(x_{N_m}) \end{pmatrix}, \tag{10}$$

$$\boldsymbol{\varphi}_{s,d} = \begin{pmatrix} \varphi_s(x_{d,1}) \\ \varphi_s(x_{d,2}) \\ \vdots \\ \varphi_s(x_{d,N_d}) \end{pmatrix}. \tag{11}$$

Consider the case when N_s velocity sensors are placed at $\tilde{x}_i$ ($i = 1,2, \ldots, N_s$) of a beam. Incorporating all the sensor outputs into the velocity vector $\mathbf{v}$, we then have

$$\mathbf{v}^{\mathrm{T}}(t) = \begin{pmatrix} \dot{\xi}(\tilde{x}_1, t) & \dot{\xi}(\tilde{x}_2, t) & \cdots & \dot{\xi}(\tilde{x}_{N_s}, t) \end{pmatrix}. \tag{12}$$

Using the eigenfunction $\varphi_k(\tilde{x}_i)$ and the associated modal coefficient $\eta_k(t)$, the velocity $\dot{\xi}(\tilde{x}_i, t)$ at $\tilde{x}_i$ of a beam is written as

$$\dot{\xi}(\tilde{x}_i, t) = \sum_{k=1}^{\infty} \varphi_k(\tilde{x}_i)\dot{\eta}_k(t). \tag{13}$$

By substituting Eq. (13) into Eq. (12), the velocity vector $\mathbf{v}$ yields

$$\mathbf{v}(t) = \tilde{\boldsymbol{\varphi}}_s \dot{\eta}_s(t) + \overline{\boldsymbol{\varphi}}_s(t), \tag{14}$$

where

$$\tilde{\boldsymbol{\varphi}}_s = \begin{pmatrix} \varphi_s(\tilde{x}_1) \\ \varphi_s(\tilde{x}_2) \\ \vdots \\ \varphi_s(\tilde{x}_{N_s}) \end{pmatrix} \tag{15}$$

and

$$\overline{\boldsymbol{\varphi}}_s(t) = \begin{pmatrix} \sum_{k=1,k\neq s}^{\infty} \varphi_k(\tilde{x}_1)\dot{\eta}_k(t) \\ \sum_{k=1,k\neq s}^{\infty} \varphi_k(\tilde{x}_2)\dot{\eta}_k(t) \\ \vdots \\ \sum_{k=1,k\neq s}^{\infty} \varphi_k(\tilde{x}_{N_s})\dot{\eta}_k(t) \end{pmatrix}. \tag{16}$$

Let the number of velocity sensors, N_s, be equal to the number of actuators, N_m, and furthermore, let the sensors and the actuators be collocated. From here on, this work deals with the case where the collocation

holds. Therefore,

$$x_i = \tilde{x}_i \quad (i = 1, 2, 3, \ldots, N_m) \tag{17}$$

and

$$\boldsymbol{\varphi}_s = \tilde{\boldsymbol{\varphi}}_s. \tag{18}$$

Next, employing a nonsingular matrix, $\mathbf{T} \in \Re^{N_m x N_m}$, the velocity vector $\mathbf{v}(t)$ may be transformed into the cluster vector $\tilde{\mathbf{v}}(t)$,

$$\tilde{\mathbf{v}}(t) = \mathbf{T}\mathbf{v}(t). \tag{19}$$

Moreover, we apply the cluster feedback to all the cluster variables $\tilde{v}_i(t)$ $(i = 1, 2, \ldots, N_m)$. For this purpose, it is necessary to obtain the cluster control vector $\tilde{\mathbf{f}}(t)$ by multiplying the cluster vector $\tilde{\mathbf{v}}(t)$ by the gain matrix $\mathbf{G} \in \Re^{N_m \, x \, N_m}$,

$$\tilde{\mathbf{f}}(t) = -\mathbf{G}\tilde{\mathbf{v}}(t), \tag{20}$$

where the gain matrix $\mathbf{G}$ is assumed to be symmetric and positive definite. Multiplying $\mathbf{T}^{\mathrm{T}}$ by the cluster control vector, the control vector $\mathbf{f}(t)$ is then given by

$$\mathbf{f}(t) = \mathbf{T}^{\mathrm{T}}\tilde{\mathbf{f}}(t) = -\mathbf{T}^{\mathrm{T}}\mathbf{G}\tilde{\mathbf{v}}(t) = -\mathbf{T}^{\mathrm{T}}\mathbf{G}\mathbf{T}\mathbf{v}(t). \tag{21}$$

Furthermore, substituting Eq. (21) into the right-hand side of Eq. (1), multiplying it by $\varphi_s(\mathbf{r})$ and integrating over the domain of the target beam yield

$$\int_0^{l_0} \varphi_s(\mathbf{r})\mathbf{f}^{\mathrm{T}}(t)\boldsymbol{\delta}\,\mathrm{d}\mathbf{r} = -\boldsymbol{\varphi}_s^{\mathrm{T}}\mathbf{T}^{\mathrm{T}}\mathbf{G}\mathbf{T}\boldsymbol{\varphi}_s\dot{\eta}_s(t) - \bar{\boldsymbol{\varphi}}_s^{\mathrm{T}}(t)\mathbf{T}^{\mathrm{T}}\mathbf{G}\mathbf{T}\boldsymbol{\varphi}_s. \tag{22}$$

Thus, the equation of motion of a beam in a modal coordinate system yields

$$\ddot{\eta}_s(t) + \boldsymbol{\varphi}_s^{\mathrm{T}}\mathbf{T}^{\mathrm{T}}\mathbf{G}\mathbf{T}\boldsymbol{\varphi}_s\dot{\eta}_s(t) + \omega_s^2\eta_s(t) = -\bar{\boldsymbol{\varphi}}_s^{\mathrm{T}}(t)\mathbf{T}^{\mathrm{T}}\mathbf{G}\mathbf{T}\boldsymbol{\varphi}_s + \mathbf{f}_d^{\mathrm{T}}(t)\boldsymbol{\varphi}_{s,d} \quad (s = 1, 2, 3, \ldots). \tag{23}$$

Consider the term, $\boldsymbol{\varphi}_s^{\mathrm{T}}\mathbf{T}^{\mathrm{T}}\mathbf{G}\mathbf{T}\boldsymbol{\varphi}_s$, on the left-hand side of Eq. (23). Because the gain matrix $\mathbf{G}$ is symmetric and positive definite, using an appropriate nonsingular matrix $\mathbf{P}$, the gain matrix may be written as

$$\mathbf{G} = \mathbf{P}^{\mathrm{T}}\mathbf{P}. \tag{24}$$

Next, substituting Eq. (24) into the term, $\boldsymbol{\varphi}_s^{\mathrm{T}}\mathbf{T}^{\mathrm{T}}\mathbf{G}\mathbf{T}\boldsymbol{\varphi}_s$, we obtain the relation

$$\boldsymbol{\varphi}_s^{\mathrm{T}}\mathbf{T}^{\mathrm{T}}\mathbf{G}\mathbf{T}\boldsymbol{\varphi}_s = \boldsymbol{\varphi}_s^{\mathrm{T}}\mathbf{T}^{\mathrm{T}}\mathbf{P}^{\mathrm{T}}\mathbf{P}\mathbf{T}\boldsymbol{\varphi}_s = \boldsymbol{\varphi}_s^{\mathrm{T}}(\mathbf{P}\mathbf{T})^{\mathrm{T}}\mathbf{P}\mathbf{T}\boldsymbol{\varphi}_s, \tag{25}$$

where the matrix $(\mathbf{P}\mathbf{T})^{\mathrm{T}}\mathbf{P}\mathbf{T}$ is obviously positive definite, so that the term $\boldsymbol{\varphi}_s^{\mathrm{T}}\mathbf{T}^{\mathrm{T}}\mathbf{G}\mathbf{T}\boldsymbol{\varphi}_s$ is positive. Negative feedback is thus achieved on every modal coordinate, providing every structural mode with damping, and hence the system is unconditionally stable. Observe that the forcing term on the right-hand side of Eq. (23) is independent of the modal coordinate, $\eta_s(t)$, and therefore has no influence on the stability of a cluster control system.

Next, replace the velocity sensors with the displacement sensors. Then the displacement vector $\boldsymbol{\xi}(t)$ is given by

$$\boldsymbol{\xi}^{\mathrm{T}}(t) = \Big(\xi(x_1, t), \quad \xi(x_2, t), \quad \ldots \quad , \xi(x_{N_m}, t) \Big). \tag{26}$$

Similarly, the equation of motion in a modal coordin ate system is derived as

$$\ddot{\eta}_s(t) + (\boldsymbol{\varphi}_s^{\mathrm{T}}\mathbf{T}^{\mathrm{T}}\mathbf{G}\mathbf{T}\boldsymbol{\varphi}_s + \omega_s^2)\eta_s(t) = -\widehat{\boldsymbol{\varphi}}_s^{\mathrm{T}}(t)\mathbf{T}^{\mathrm{T}}\mathbf{G}\mathbf{T}\boldsymbol{\varphi}_s + \mathbf{f}_d^{\mathrm{T}}(t)\boldsymbol{\varphi}_{s,d} \quad (s = 1, 2, 3, \ldots), \tag{27}$$

where

$$\widehat{\boldsymbol{\varphi}}_s = \begin{pmatrix} \sum_{k=1,k\neq s}^{\infty} \varphi_k(x_1)\eta_k(t) \\ \sum_{k=1,k\neq s}^{\infty} \varphi_k(x_2)\eta_k(t) \\ \vdots \\ \sum_{k=1,k\neq s}^{\infty} \varphi_k(x_n)\eta_k(t) \end{pmatrix}. \tag{28}$$

As is clear from Eq. (27), the cluster feedback via displacement sensor outputs enhances modal rigidity. In this case, although the gain margin is infinite, the phase margin is close to zero, and hence the control system is marginally stable.

3. Cluster vector-based control for generating a vibration-free state

3.1. Cluster filtering and cluster actuation

Supposing that a beam is harmonically oscillating, its displacement will be of the form

$$\xi(x,t) = \xi(x)\mathrm{e}^{\mathrm{j}\omega t}, \tag{29}$$

where

$$\xi(x) = \sum_{k=1}^{\infty} \varphi_k(x)\eta_k \approx \boldsymbol{\varphi}^{\mathrm{T}}(x)\boldsymbol{\eta} \tag{30}$$

and where the eigenfunction vector $\boldsymbol{\varphi}$ and the modal amplitude vector $\boldsymbol{\eta}$ are defined as

$$\boldsymbol{\varphi}(x) = \mathrm{col}(\varphi_1(x), \varphi_2(x), \ldots, \varphi_N(x)) \in \Re^N, \tag{31}$$

$$\boldsymbol{\eta} = \mathrm{col}(\eta_1, \eta_2, \ldots, \eta_N) \in \mathfrak{C}^N, \tag{32}$$

where $N \gg 1$. Using Eq. (9), the modal amplitude vector may be expressed as

$$\boldsymbol{\eta} = \boldsymbol{\Lambda}_\omega(\boldsymbol{\Phi}\mathbf{f} + \boldsymbol{\Phi}_d\mathbf{f}_d), \tag{33}$$

where

$$\boldsymbol{\Lambda}_\omega = \begin{pmatrix} \dfrac{1}{\omega_1^2-\omega^2} & 0 & \cdots & 0 \\ 0 & \dfrac{1}{\omega_2^2-\omega^2} & 0 & \vdots \\ \vdots & 0 & \ddots & 0 \\ 0 & \cdots & \cdots & \dfrac{1}{\omega_N^2-\omega^2} \end{pmatrix} \in \Re^{N\times N}, \tag{34}$$

$$\boldsymbol{\Phi} = \begin{pmatrix} \varphi_1(x_1) & \varphi_1(x_2) & \cdots & \varphi_1(x_{N_m}) \\ \varphi_2(x_1) & \varphi_2(x_2) & \cdots & \varphi_2(x_{N_m}) \\ \vdots & \vdots & \cdots & \vdots \\ \varphi_N(x_1) & \varphi_N(x_2) & \cdots & \varphi_N(x_{N_m}) \end{pmatrix} = \begin{pmatrix} \boldsymbol{\varphi}_1^{\mathrm{T}} \\ \boldsymbol{\varphi}_2^{\mathrm{T}} \\ \vdots \\ \boldsymbol{\varphi}_N^{\mathrm{T}} \end{pmatrix} \in \Re^{N\times N_m}, \tag{35}$$

$$\mathbf{\Phi}_d = \begin{pmatrix} \varphi_1(x_{d,1}) & \varphi_1(x_{d,2}) & \cdots & \varphi_1(x_{d,N_d}) \\ \varphi_2(x_{d,1}) & \varphi_2(x_{d,2}) & \cdots & \varphi_2(x_{d,N_d}) \\ \vdots & \vdots & \cdots & \vdots \\ \varphi_N(x_{d,1}) & \varphi_N(x_{d,2}) & \cdots & \varphi_N(x_{d,N_d}) \end{pmatrix} = \begin{pmatrix} \boldsymbol{\varphi}_{d,1}^{\mathrm{T}} \\ \boldsymbol{\varphi}_{d,2}^{\mathrm{T}} \\ \vdots \\ \boldsymbol{\varphi}_{d,N}^{\mathrm{T}} \end{pmatrix} \in \Re^{N \times N_d}. \tag{36}$$

Furthermore, the displacement vector in Eq. (26) is expressed as

$$\boldsymbol{\xi} = \mathbf{\Phi}^{\mathrm{T}} \boldsymbol{\eta} \in \Re^{N_m}, \tag{37}$$

so that

$$\boldsymbol{\xi} = \mathbf{\Omega}_{\omega} \mathbf{f} + \mathbf{\Omega}_{\omega,d} \mathbf{f}_d, \tag{38}$$

where

$$\mathbf{\Omega}_{\omega} = \mathbf{\Phi}^{\mathrm{T}} \mathbf{\Lambda}_{\omega} \mathbf{\Phi} \in \Re^{N_m x N_m}, \tag{39}$$

$$\mathbf{\Omega}_{\omega,d} = \mathbf{\Phi}^{\mathrm{T}} \mathbf{\Lambda}_{\omega} \mathbf{\Phi}_d \in \Re^{N_m x N_d}. \tag{40}$$

To generate a vibration-free state in the designated area of a target beam, this paper introduces cluster control. For that purpose, all the governing parameters of a beam, i.e. $\xi(x)$, $\theta(x)$, $m_x(x)$ and $q_x(x)$, need to be measured by cluster filtering [13]. However, three out of the four parameters, i.e. $\theta(x)$, $m_x(x)$ and $q_x(x)$, are not easy to measure in practice, and hence a finite difference method is used to extract these variables. First, the three parameters are defined as:

$$\theta(x) = \frac{\mathrm{d}\xi(x)}{\mathrm{d}x}, \tag{41}$$

$$m_x(x) = \frac{\mathrm{d}\theta(x)}{\mathrm{d}x} = \frac{\mathrm{d}^2\xi(x)}{\mathrm{d}x^2}, \tag{42}$$

$$q_x(x) = \frac{\mathrm{d}m_x(x)}{\mathrm{d}x} = \frac{\mathrm{d}^3\xi(x)}{\mathrm{d}x^3}. \tag{43}$$

Furthermore, Eqs. (41)–(43) may approximately be expressed as:

$$\theta(x) = \frac{\xi(x+\Delta) - \xi(x)}{\Delta}, \tag{44}$$

$$m_x(x) = \frac{\xi(x+2\Delta) - 2\xi(x+\Delta) + \xi(x)}{\Delta^2}, \tag{45}$$

$$q_x(x) = \frac{\xi(x+3\Delta) - 3\xi(x+2\Delta) + 3\xi(x+\Delta) - \xi(x)}{\Delta^3} \tag{46}$$

where Δ is a sensing interval.

Next, introducing the transformation matrix $\mathbf{L}$, the relationship between the displacement vector $\boldsymbol{\xi}$ and the transformed vector $\hat{\boldsymbol{\xi}}$, for estimating the four dominant state variables, may be expressed as

$$\hat{\boldsymbol{\xi}} = \mathbf{L}^{\mathrm{T}} \boldsymbol{\xi}, \tag{47}$$

where

$$\hat{\boldsymbol{\xi}} = \begin{pmatrix} \hat{\xi}(x) \\ \hat{\theta}(x) \\ \hat{m}_x(x) \\ \hat{q}_x(x) \end{pmatrix}, \tag{48}$$

$$\boldsymbol{\xi} = \begin{pmatrix} \xi(x) \\ \xi(x+\Delta) \\ \xi(x+2\Delta) \\ \xi(x+3\Delta) \end{pmatrix}, \tag{49}$$

$$\mathbf{L}^{\mathrm{T}} = \begin{pmatrix} 1 & 0 & 0 & 0 \\ -1/\Delta & 1/\Delta & 0 & 0 \\ 1/\Delta^2 & -2/\Delta^2 & 1/\Delta^2 & 0 \\ -1/\Delta^3 & 3/\Delta^3 & -3/\Delta^3 & 1/\Delta^3 \end{pmatrix}. \tag{50}$$

It should be noted that the transformed vector $\hat{\boldsymbol{\xi}}$ is not the cluster vector (to be discussed later), and therefore, the vector $\hat{\boldsymbol{\xi}}$ further needs to be transformed using a nonsingular transformation matrix $\mathbf{T}_0$. Hence, it follows that

$$\tilde{\boldsymbol{\xi}} = \begin{pmatrix} \tilde{\xi}_1 \\ \tilde{\xi}_2 \\ \tilde{\xi}_3 \\ \tilde{\xi}_4 \end{pmatrix} = \mathbf{T}_0^{\mathrm{T}} \hat{\boldsymbol{\xi}}. \tag{51}$$

Here, the transformed vector, $\tilde{\boldsymbol{\xi}}$, is the cluster vector as shown later. The ith element, $\tilde{\xi}_i$, of the cluster vector $\tilde{\boldsymbol{\xi}}$ is then independently assigned with a feedback gain G_i, so that the cluster control force vector $\tilde{\mathbf{f}}$ corresponding to the cluster vector $\tilde{\boldsymbol{\xi}}$ is given by

$$\tilde{\mathbf{f}} = \begin{pmatrix} \tilde{f}_1 \\ \tilde{f}_2 \\ \tilde{f}_3 \\ \tilde{f}_4 \end{pmatrix} = -\boldsymbol{\Lambda}_G \tilde{\boldsymbol{\xi}}, \tag{52}$$

where $\boldsymbol{\Lambda}_G$ is the gain matrix defined as

$$\boldsymbol{\Lambda}_G = \begin{pmatrix} G_1 & 0 & 0 & 0 \\ 0 & G_2 & 0 & 0 \\ 0 & 0 & G_3 & 0 \\ 0 & 0 & 0 & G_4 \end{pmatrix}. \tag{53}$$

Cluster actuation [13] is performed in the same way as cluster filtering. The cluster actuation vector $\tilde{\mathbf{f}}$ is then transformed into $\hat{\mathbf{f}}$, i.e. the counterpart of the transformed vector $\hat{\boldsymbol{\xi}}$. Hence, it follows that

$$\hat{\mathbf{f}} = \begin{pmatrix} \hat{f}_1 \\ \hat{f}_2 \\ \hat{f}_3 \\ \hat{f}_4 \end{pmatrix} = \mathbf{T}_0 \tilde{\mathbf{f}}. \tag{54}$$

Furthermore, the transformed vector $\hat{\mathbf{f}}$ is transformed back into the control force vector $\mathbf{f}$ in a real system. Therefore,

$$\mathbf{f} = \begin{pmatrix} f_1 \\ f_2 \\ f_3 \\ f_4 \end{pmatrix} = \mathbf{L} \hat{\mathbf{f}}. \tag{55}$$

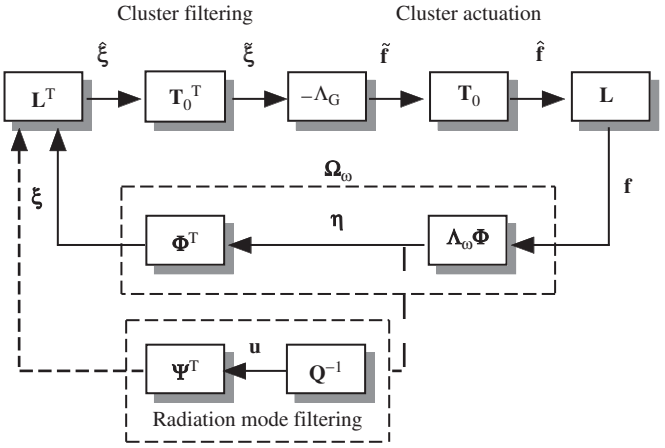

Fig. 1. Block diagram of a cluster feedback control system for generating a vibration-free state; dashed line shows a signal flow in terms of the radiation (power) mode filtering.

Fig. 1 shows the block diagram of a cluster feedback control system illustrating the following steps: (1) measurement of a beam in real space, (2) cluster filtering, (3) cluster control, (4) cluster actuation and (5) actuation of beam in real space. Note that disturbance forces are excluded from the diagram, because they are independent of feedback control. Based on the figure, it is worth discussing which vector may be the cluster vector that enables independent control of each cluster without causing spillover. Once the cluster vector is identified, it becomes possible to simplify the control system. The control system may then be altered from a multiple-input multiple-output (MIMO) system to a multiple single-input single-output (SISO) system, thus significantly reducing the control task burden.

3.2. Cluster vector

Consider a feedback control loop consisting of the state vectors $\mathbf{z}_i$ and transfer matrices $\mathbf{T}_{ij}$. A loop-gain matrix starting from the ith state vector $\mathbf{z}_i$ to itself may be expressed as

$$\tilde{\mathbf{T}}_i = \mathbf{T}_{i,i-1}\mathbf{T}_{i-1,i-2}\cdots\mathbf{T}_{i+1,i}. \tag{56}$$

Therefore, the state equation from $\mathbf{z}_i$ to $\mathbf{z}_i$ becomes

$$\mathbf{z}_i = \tilde{\mathbf{T}}_i\mathbf{z}_i. \tag{57}$$

If the loop-gain matrix $\tilde{\mathbf{T}}_i$ is diagonal, then the associated vector $\mathbf{z}_i$ is defined as the *cluster vector*. If this is the case, Eq. (57) will be of the form

$$\begin{aligned}\mathbf{z}_i &= \begin{pmatrix} z_1 \\ z_2 \\ \vdots \\ z_N \end{pmatrix} = \begin{pmatrix} \Lambda_{T,1} & & & 0 \\ & \Lambda_{T,2} & & \\ & & \ddots & \\ 0 & & & \Lambda_{T,N} \end{pmatrix} \begin{pmatrix} z_1 \\ z_2 \\ \vdots \\ z_N \end{pmatrix} \\ &= \mathbf{\Lambda}_T\mathbf{z}_i. \end{aligned} \tag{58}$$

Therefore, the ith element z_i of the vector $\mathbf{z}_i$ is related only to its own element through the transmittance $\Lambda_{T,i}$. As mentioned before, once the cluster vector is found, the feedback control system may be restructured from a MIMO system to a cluster control system—a multi SISO system with input vector $\mathbf{z}_{i+1}$ and output vector $\mathbf{z}_i$.

Consider a control loop that consists of N state vectors and N transfer matrices. Depending on the state vectors that are employed as input and output vectors, there are N possible combinations of a loop-gain matrix. Hence, among N loop-gain matrices, if the resultant matrix is found to be diagonal, the associated

vector is the cluster vector. For instance, in the case of a beam, four dominant variables—$\xi(x)$, $\theta(x)$, $m(x)$ and $q_x(x)$—uniquely resolve the dynamical behavior of the beam; however, the vector $\hat{\boldsymbol{\xi}}$ consisting of the four parameters is not the cluster vector, as shown later.

Case 1: Is the displacement vector $\boldsymbol{\xi}$ the cluster vector?

With reference to Fig. 1, consider a loop-gain matrix of a feedback control system starting from $\boldsymbol{\xi}$ to itself, $\boldsymbol{\xi}$. The displacement vector $\boldsymbol{\xi}$ may then be expressed as

$$\begin{aligned}\boldsymbol{\xi} &= -\boldsymbol{\Omega}_\omega \mathbf{L}\mathbf{T}_0\boldsymbol{\Lambda}_G\mathbf{T}_0^{\mathrm{T}}\mathbf{L}^{\mathrm{T}}\boldsymbol{\xi}\\ &= -\boldsymbol{\Omega}_\omega \mathbf{f}.\end{aligned} \tag{59}$$

Note that among the matrices in Eq. (59), only the matrix $\mathbf{T}_0$ is adjustable whereas the others have already been defined. Therefore, it is not possible for $\boldsymbol{\Omega}_\omega\mathbf{L}\mathbf{T}_0\boldsymbol{\Lambda}_G\mathbf{T}_0^{\mathrm{T}}\mathbf{L}^{\mathrm{T}}$ to be a diagonal matrix, and hence, the vector $\boldsymbol{\xi}$ cannot be the cluster vector. In addition, matrix $\boldsymbol{\Omega}_\omega$ is symmetric but not diagonal; therefore, there are crosstalk transmittances from an element of $\mathbf{f}$ to the respective elements of the displacement vector $\boldsymbol{\xi}$.

Case 2: Is the transformed displacement vector $\hat{\boldsymbol{\xi}}$ the cluster vector?

Using a loop-gain matrix starting from the transformed displacement vector $\hat{\boldsymbol{\xi}}$ to itself, the vector $\hat{\boldsymbol{\xi}}$ may be expressed as

$$\begin{aligned}\hat{\boldsymbol{\xi}} &= -\mathbf{L}^{\mathrm{T}}\boldsymbol{\Omega}_\omega \mathbf{L}\mathbf{T}_0\boldsymbol{\Lambda}_G\mathbf{T}_0^{\mathrm{T}}\hat{\boldsymbol{\xi}}\\ &= -\mathbf{L}^{\mathrm{T}}\boldsymbol{\Omega}_\omega \mathbf{L}\hat{\mathbf{f}}.\end{aligned} \tag{60}$$

If the transformation matrix $\mathbf{L}$ was adjustable, it would allow the symmetric matrix $\boldsymbol{\Omega}_\omega$ to be diagonal; hence, $\hat{\boldsymbol{\xi}}$ would be the cluster vector. However, the matrix $\mathbf{L}$ is resolved as a finite difference matrix and is therefore unable to diagonalize the matrix $\boldsymbol{\Omega}_\omega$. Thus, the ith control force $\hat{f}_i$ of $\hat{\mathbf{f}}$ excites the elements of the vector $\hat{\boldsymbol{\xi}}$.

Case 3: Is the transformed vector $\tilde{\boldsymbol{\xi}}$ the cluster vector?

A loop-gain matrix starting from the transformed vector $\tilde{\boldsymbol{\xi}}$ to itself may be expressed as

$$\begin{aligned}\tilde{\boldsymbol{\xi}} &= -\mathbf{T}_0^{\mathrm{T}}\mathbf{L}^{\mathrm{T}}\boldsymbol{\Omega}_\omega \mathbf{L}\mathbf{T}_0\boldsymbol{\Lambda}_G\tilde{\boldsymbol{\xi}}\\ &= -\mathbf{T}_0^{\mathrm{T}}\mathbf{L}^{\mathrm{T}}\boldsymbol{\Omega}_\omega \mathbf{L}\mathbf{T}_0\tilde{\mathbf{f}}.\end{aligned} \tag{61}$$

Now that the matrix $\mathbf{L}^{\mathrm{T}}\boldsymbol{\Omega}_\omega\mathbf{L}$ is symmetric (recall that $\boldsymbol{\Lambda}_G$ is diagonal; therefore, it can be omitted in the current discussion), an appropriate orthogonal matrix $\mathbf{T}_0$ is able to diagonalize $\mathbf{L}^{\mathrm{T}}\boldsymbol{\Omega}_\omega\mathbf{L}$, and hence the transformed vector $\tilde{\boldsymbol{\xi}}$ can be the cluster vector. If this is the case, the ith element of the force vector $\tilde{\mathbf{f}}$ excites *only* the ith element of the transformed vector $\tilde{\boldsymbol{\xi}}$ without causing control spillover, i.e.

$$\begin{aligned}\tilde{\boldsymbol{\xi}} &= \begin{pmatrix}\tilde{\xi}_1\\ \tilde{\xi}_2\\ \tilde{\xi}_3\\ \tilde{\xi}_4\end{pmatrix} = -\begin{pmatrix}\Theta_1(\omega) & 0 & 0 & 0\\ 0 & \Theta_2(\omega) & 0 & 0\\ 0 & 0 & \Theta_3(\omega) & 0\\ 0 & 0 & 0 & \Theta_4(\omega)\end{pmatrix}\begin{pmatrix}\tilde{f}_1\\ \tilde{f}_2\\ \tilde{f}_3\\ \tilde{f}_4\end{pmatrix}\\ &= -\boldsymbol{\Lambda}_\Theta\tilde{\mathbf{f}}.\end{aligned} \tag{62}$$

Using Eq. (52), Eq. (62) further expands to

$$\begin{aligned}\tilde{\boldsymbol{\xi}} &= -\boldsymbol{\Lambda}_\Theta\tilde{\mathbf{f}}\\ &= -\boldsymbol{\Lambda}_\Theta\boldsymbol{\Lambda}_G\tilde{\boldsymbol{\xi}}\\ &= -\begin{pmatrix}G_1\Theta_1(\omega) & 0 & 0 & 0\\ 0 & G_2\Theta_2(\omega) & 0 & 0\\ 0 & 0 & G_3\Theta_3(\omega) & 0\\ 0 & 0 & 0 & G_4\Theta_4(\omega)\end{pmatrix}\begin{pmatrix}\tilde{\xi}_1\\ \tilde{\xi}_2\\ \tilde{\xi}_3\\ \tilde{\xi}_4\end{pmatrix}\\ &= -\boldsymbol{\Lambda}_{\Theta G}\tilde{\boldsymbol{\xi}}.\end{aligned} \tag{63}$$

Thus, by introducing cluster filtering and cluster actuation, a MIMO control system with four inputs and four outputs may be decoupled into four SISO control systems, thereby significantly reducing the signal-processing burden handled during control. As such, the eigenpairs in each cluster may be independently resolved, thus avoiding spillover.

3.3. State equation of a cluster control system

Consider a beam element, as shown in Fig. 2, with the node number i and $i-1$ at the right and left ends of the beam element, respectively. Using the transfer matrix $\mathbf{T}_{i,i-1}$, which bridges these two nodes, the relation between the state vector $\mathbf{z}_i(x_i)$ and $\mathbf{z}_i(x_{i-1})$ abbreviated as $\mathbf{z}_i$ and $\mathbf{z}_{i-1}$, respectively, is expressed by

$$\mathbf{z}_i = \mathbf{T}_{i,i-1}(\delta_i)\mathbf{z}_{i-1}, \tag{64}$$

where

$$\mathbf{T}_{i,i-1}(\delta_i) = \begin{pmatrix} t_1 & t_4 & t_3 & t_2 \\ k^4 t_2 & t_1 & t_4 & t_3 \\ k^4 t_3 & k^4 t_2 & t_1 & t_4 \\ k^4 t_4 & k^4 t_3 & k^4 t_2 & t_1 \end{pmatrix}, \tag{65}$$

where

$$k = \left(\frac{\rho A \omega^2}{EI}\right)^{\frac{1}{4}} \tag{66}$$

and where

$$t_1 = (\mathrm{e}^{-\mathrm{j}k\delta_i} + \mathrm{e}^{-k\delta_i} + \mathrm{e}^{\mathrm{j}k\delta_i} + \mathrm{e}^{k\delta_i})/4, \tag{67a}$$

$$t_2 = (-j\mathrm{e}^{-\mathrm{j}k\delta_i} - \mathrm{e}^{-k\delta_i} + j\mathrm{e}^{\mathrm{j}k\delta_i} + \mathrm{e}^{k\delta_i})/4k^3, \tag{67b}$$

$$t_3 = (-\mathrm{e}^{-\mathrm{j}k\delta_i} + \mathrm{e}^{-k\delta_i} - \mathrm{e}^{\mathrm{j}k\delta_i} + \mathrm{e}^{k\delta_i})/4k^2, \tag{67c}$$

$$t_4 = (j\mathrm{e}^{-\mathrm{j}k\delta_i} - \mathrm{e}^{-k\delta_i} - j\mathrm{e}^{\mathrm{j}k\delta_i} + \mathrm{e}^{k\delta_i})/4k. \tag{67d}$$

Then, the state equation of a beam where N_m point forces act is given by

$$\mathbf{z}_R = \mathbf{T}_{RL}\mathbf{z}_L + \sum_{i=1}^{N_m} \mathbf{T}_{Ri}\mathbf{f}_i \tag{68}$$

where

$$\mathbf{f}_i^{\mathrm{T}} = \begin{pmatrix} 0 & 0 & 0 & f_i/EI \end{pmatrix}. \tag{69}$$

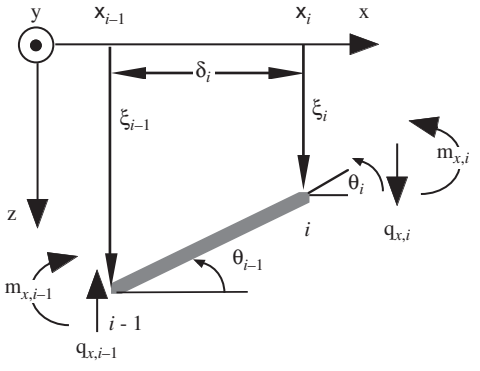

Fig. 2. Beam element and internal forces.

Next, the boundary conditions at both ends of the beam, R and L, are determined by setting two out of the four variables in the state vector equal to zero. Consider the case when the ith and jth elements of $\mathbf{z}_R$ are set equal to zero, whereas the mth and nth elements of $\mathbf{z}_L$ are set to be nonzero. For instance, a set of $m=3$, $n=4$, $i=1$ and $j=2$ expresses the case of a cantilever beam with the left end clamped. Eq. (64) further expands to:

$$0_i = {}_{RL}t_{im}z_{Lm} + {}_{RL}t_{in}z_{Ln} + \frac{1}{EI}\sum_{k=1}^{N_m} {}_{Rk}t_{i4}f_k, \tag{70}$$

$$0_j = {}_{RL}t_{jm}z_{Lm} + {}_{RL}t_{jn}z_{Ln} + \frac{1}{EI}\sum_{k=1}^{N_m} {}_{Rk}t_{j4}f_k, \tag{71}$$

where 0_i and ${}_{ij}t_{kl}$ denote zero of the ith element of the vector, and the kth and lth element of the transfer matrix $\mathbf{T}_{ij}$, respectively. From Eq. (66), the elements z_{Lm} and z_{Ln} of the state vector $\mathbf{z}_L$ are written as

$$z_{Lm} = -\frac{1}{EI\Delta_{ch}}\left({}_{RL}t_{jn}\sum_{k=1}^{N_m} {}_{Rk}t_{i4}f_k - {}_{RL}t_{in}\sum_{k=1}^{N_m} {}_{Rk}t_{j4}f_k\right), \tag{72}$$

$$z_{Lm} = -\frac{1}{EI\Delta_{ch}}\left(-{}_{RL}t_{jm}\sum_{k=1}^{N_m} {}_{Rk}t_{i4}f_k + {}_{RL}t_{im}\sum_{k=1}^{N_m} {}_{Rk}t_{j4}f_k\right), \tag{73}$$

where

$$\Delta_{ch} = {}_{RL}t_{im}{}_{RL}t_{jn} - {}_{RL}t_{in}{}_{RL}t_{jm}. \tag{74}$$

As the initial vector $\mathbf{z}_L$ is obtained from Eqs. (70) and (74), the state vector $\mathbf{z}_x$ at x of the beam may be determined uniquely.

Fig. 3 illustrates the signal flow diagram of a cluster control system designated to control the four state variables of a beam: $\xi(x)$, $\theta(x)$, $m_x(x)$ and $q_x(x)$, which uniquely govern the system equation of a beam subjected to four collocated point sensors/actuators. Supposing that the beam is subjected to a disturbance force f_d acting at x_d, the state equation at x in the figure is then written as

$$\mathbf{z}_x = \mathbf{T}_{x,L}\mathbf{z}_L + \mathbf{T}_{x,1}\mathbf{f}_1 + \mathbf{T}_{x,2}\mathbf{f}_2 + \mathbf{T}_{x,3}\mathbf{f}_3 + \mathbf{T}_{x,4}\mathbf{f}_4. \tag{75}$$

3.4. Vibration-free node

It is worth discussing the physical meaning of a vibration-free state. Fig. 4 illustrates the time histories of the four state variables (i.e. dominant parameters that uniquely resolve the dynamic behavior of a clamped–clamped beam) excited at the third modal frequency. Table 1 lists the beam specifications. Observe that two nodes appear in the time histories of the displacement response of the beam; nodes are normally considered vibration-free. Thus, in some industries there have been attempts to avoid vibration by designing such that a node position intentionally coincides with the grip location of a hand-tool. It is true that when placing an accelerometer at a node, the sensor output becomes small enough; however, the node is not vibration-free. A vibration-free state means that all the four state variables dominating the dynamical characteristics of a beam must be null. Similarly, a 'vibration-free node' denotes that all the elements of the corresponding state vector are zero.

We now consider the benefits of generating a vibration-free node. Consider a beam's state vectors $\mathbf{z}_i$ and $\mathbf{z}_j$ at 'i' and 'j', respectively. Using a transfer matrix $\mathbf{T}_{ji}$, which connects both state vectors, the state vector $\mathbf{z}_j$ is given by

$$\mathbf{z}_j = \mathbf{T}_{ji}\mathbf{z}_i. \tag{76}$$

If the state vector $\mathbf{z}_i$ is a null vector, the node at "i" is vibration-free. Then, the state vector $\mathbf{z}_j$ at "j" apparently becomes a null vector, thus implying that the region between the points "i" and "j" is also vibration-free.

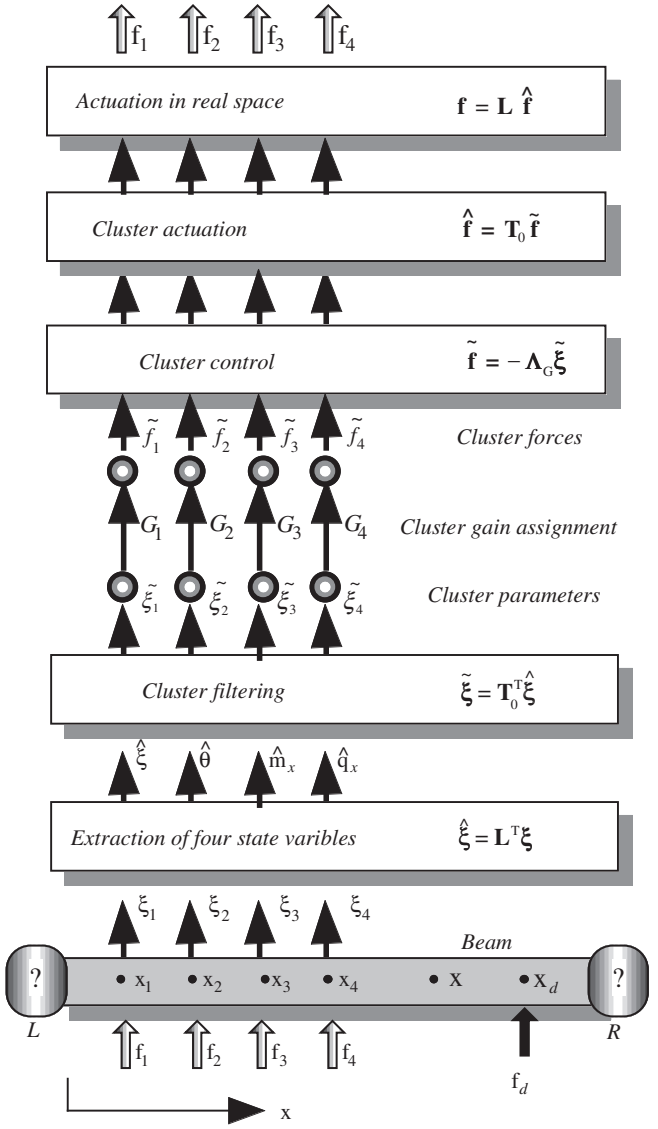

Fig. 3. Signal flow of cluster control of a beam for generating a vibration-free state.

Therefore, generating a vibration-free node at a designated location enables one to produce a vibration-free state around the designated point. Similarly, the so-called node where both $\xi(x)$ and $m_x(x)$ are zero seems to be vibration-free; however, the other state variables, $\theta(x)$ and $q_x(x)$, are nonzero. Hence, the state vector at the node is not vibration-free but only bridges opposite sides of the node for transferring structural waves.

We now consider how the above-mentioned method differs from DVFB [18,19] with an extremely high feedback gain applied at a sensor/actuator collocated location. This is clarified by considering the difference between the so-called node and a vibration-free node. Because conventional active vibration control, including DVFB, simply produces a node at a sensor/actuator location, a vibration-free state may not be realized. Even with the introduction of control performance for minimizing the kinetic energy of a beam, a vibration-free state may not be generated, because a completely vibration-free state is beyond the scope of the design.

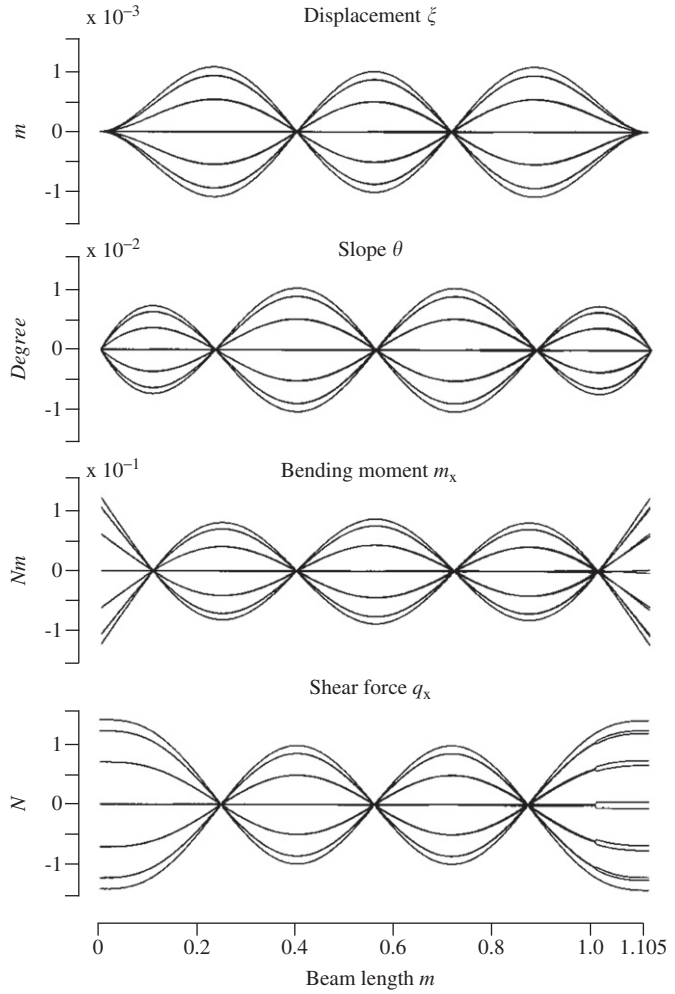

Fig. 4. Time histories of four state variables of a clamped–clamped beam excited at the third modal frequency.

Table 1
Dimensions of a clamped–clamped beam used in numerical analysis and experiment

Total length	Thickness	Width
1.105 m	1.5 mm	4.5 cm
Young's modulus	Density	Material
7.4×10^{10} N/m^2	2770 kg/m^3	Duralumin

3.5. Performance index

Now that we know how to generate a vibration-free state in the designated region of the target beam, a vibration-free node needs to be produced at x, the designated control point of a beam. Consequently, dominant variables, $\xi(x)$, $\theta(x)$, $m_x(x)$ and $q_x(x)$, are to be extracted and suppressed. Therefore, the performance index J, needed to achieve the vibration-free state, is defined as

$$J = \hat{\boldsymbol{\xi}}^H \hat{\boldsymbol{\xi}} = \hat{\xi}^2 + \hat{\theta}^2 + \hat{m}_x^2 + \hat{q}_x^2. \tag{77}$$

Because all the elements of the vector $\hat{\boldsymbol{\xi}}$ are dominant factors that uniquely resolve the dynamic behavior of a beam, the performance index consisting of all the four elements in Eq. (77) needs to be minimized.

Minimization of the performance index, defined to evaluate a vibration-free state, is performed from the viewpoint of the cluster vector. For this purpose, the cluster vector must be connected to both cluster filtering and cluster actuation. From Eq. (38), $\hat{\boldsymbol{\xi}}$ is written as

$$\hat{\boldsymbol{\xi}} = \mathbf{L}^{\mathrm{T}}\boldsymbol{\xi} = \mathbf{L}^{\mathrm{T}}(-\boldsymbol{\Omega}_{\omega}\mathbf{f} + \boldsymbol{\Omega}_{\omega,d}\mathbf{f}_d). \tag{78}$$

Using Eq. (60), $\hat{\boldsymbol{\xi}}$ further expands to

$$\begin{aligned}\hat{\boldsymbol{\xi}} &= \mathbf{L}^{\mathrm{T}}(-\boldsymbol{\Omega}_{\omega}\mathbf{L}\mathbf{T}_0\boldsymbol{\Lambda}_G\mathbf{T}_0^{\mathrm{T}}\mathbf{L}^{\mathrm{T}}\boldsymbol{\xi} + \boldsymbol{\Omega}_{\omega,d}\mathbf{f}_d)\\ &= \mathbf{L}^{\mathrm{T}}(-\boldsymbol{\Omega}_{\omega}\mathbf{L}\mathbf{T}_0\boldsymbol{\Lambda}_G\mathbf{T}_0^{\mathrm{T}}\hat{\boldsymbol{\xi}} + \boldsymbol{\Omega}_{\omega,d}\mathbf{f}_d),\end{aligned} \tag{79}$$

so that

$$\hat{\boldsymbol{\xi}} = (\mathbf{I} + \mathbf{L}^{\mathrm{T}}\boldsymbol{\Omega}_{\omega}\mathbf{L}\mathbf{T}_0\boldsymbol{\Lambda}_G\mathbf{T}_0^{\mathrm{T}})^{-1}\mathbf{L}^{\mathrm{T}}\boldsymbol{\Lambda}\boldsymbol{\Omega}_{\omega,d}\mathbf{f}_d. \tag{80}$$

As stated before, $\hat{\boldsymbol{\xi}}$ is not the cluster vector. The matrix term $(\mathbf{I} + \mathbf{L}^{\mathrm{T}}\boldsymbol{\Omega}_{\omega}\mathbf{L}\mathbf{T}_0\boldsymbol{\Lambda}_G\mathbf{T}_0^{\mathrm{T}})$ on the right-hand side of Eq. (80) is not diagonal; therefore, it is not certain whether the suppression of the elements of $\hat{\boldsymbol{\xi}}$ may directly lead to the suppression of the performance index due to the matrix cross terms involved. According to Eq. (77), the performance index is expressed by summing up the squares of the four variables. Thus, the suppression of each term is likely to decrease the performance index. However, this is not always true. Because the vector $\hat{\boldsymbol{\xi}}$ is not the cluster vector, the suppression of one term might increase the other terms, as they are not independent of each other. This is easily deduced from the time histories of the four state variables of a beam, as shown in Fig. 4. The location of the maximum absolute value of the deflection coincides with that of the minimum absolute value of the slope; hence, the suppression of $\xi(x)$ does not necessarily lead to the suppression of $\theta(x)$.

With this in mind, consider the cluster vector $\tilde{\boldsymbol{\xi}}$, which is expressed as

$$\tilde{\boldsymbol{\xi}} = -\mathbf{T}_0^{\mathrm{T}}\mathbf{L}^{\mathrm{T}}\boldsymbol{\Omega}_{\omega}\mathbf{L}\mathbf{T}_0\boldsymbol{\Lambda}_G\tilde{\boldsymbol{\xi}} + \mathbf{T}_0^{\mathrm{T}}\mathbf{L}^{\mathrm{T}}\boldsymbol{\Omega}_{\omega,d}\mathbf{f}_d. \tag{81}$$

Hence, it follows that

$$\tilde{\boldsymbol{\xi}} = (\mathbf{I} + \mathbf{T}_0^{\mathrm{T}}\mathbf{L}^{\mathrm{T}}\boldsymbol{\Omega}_{\omega}\mathbf{L}\mathbf{T}_0\boldsymbol{\Lambda}_G)^{-1}\mathbf{T}_0^{\mathrm{T}}\mathbf{L}^{\mathrm{T}}\boldsymbol{\Omega}_{\omega,d}\mathbf{f}_d. \tag{82}$$

Because $\tilde{\boldsymbol{\xi}}$ is the cluster vector, Eq. (82) further expands to

$$\begin{aligned}\tilde{\boldsymbol{\xi}} &= (\mathbf{I} + \boldsymbol{\Lambda}_{\Theta G})^{-1}\mathbf{T}_0^{\mathrm{T}}\mathbf{L}^{\mathrm{T}}\boldsymbol{\Omega}_{\omega,d}\mathbf{f}_d\\ &= \overline{\boldsymbol{\Lambda}}_{\Theta G}\mathbf{T}_0^{\mathrm{T}}\mathbf{L}^{\mathrm{T}}\boldsymbol{\Omega}_{\omega,d}\mathbf{f}_d,\end{aligned} \tag{83}$$

where

$$\begin{aligned}\overline{\boldsymbol{\Lambda}}_{\Theta G} &= (\mathbf{I} + \boldsymbol{\Lambda}_{\Theta G})^{-1}\\ &= \begin{pmatrix} 1/(1+G_1\Theta_1(\omega)) & 0 & 0 & 0\\ 0 & 1/(1+G_2\Theta_2(\omega)) & 0 & 0\\ 0 & 0 & 1/(1+G_3\Theta_3(\omega)) & 0\\ 0 & 0 & 0 & 1/(1+G_4\Theta_4(\omega)) \end{pmatrix}.\end{aligned} \tag{84}$$

Note that the matrix term $\mathbf{T}_0^{\mathrm{T}}\mathbf{L}^{\mathrm{T}}\boldsymbol{\Omega}_{\omega,d}\mathbf{f}_d$ in Eq. (83), resolved in terms of disturbance forces, is independent of control, and hence *only* the diagonal matrix $\overline{\boldsymbol{\Lambda}}_{\Theta G}$ is responsible for attenuating the performance index.

Recall that the transformed displacement vector $\hat{\boldsymbol{\xi}}$ is related to $\tilde{\boldsymbol{\xi}}$ by the following relation:

$$\hat{\boldsymbol{\xi}} = \mathbf{T}_0\tilde{\boldsymbol{\xi}}, \tag{85}$$

where $\mathbf{T}_0$ is the orthogonal matrix. Therefore, the performance index J yields

$$\begin{aligned} J &= \hat{\boldsymbol{\xi}}^H \hat{\boldsymbol{\xi}} = \hat{\xi}^2 + \hat{\theta}^2 + \hat{m}_x^2 + \hat{q}_x^2 \\ &= \tilde{\boldsymbol{\xi}}^H \mathbf{T}_0^{\mathrm{T}} \mathbf{T}_0 \tilde{\boldsymbol{\xi}} \\ &= \tilde{\boldsymbol{\xi}}^H \tilde{\boldsymbol{\xi}} = \tilde{\xi}_1^2 + \tilde{\xi}_2^2 + \tilde{\xi}_3^2 + \tilde{\xi}_4^2. \end{aligned} \tag{86}$$

Apparently, from Eq. (86), the suppression of the squared cluster elements, $\tilde{\xi}_i^2$ ($i = 1, 2, 3, 4$), of the cluster vector $\tilde{\boldsymbol{\xi}}$ definitely leads to the suppression of the performance index J, thereby generating a vibration-free state in the target region of a beam without causing spillover via $\tilde{f}_i$, as expressed in Eq. (62). In this case, the suppression of $\tilde{\xi}_i$ implies the attenuation of $1/(1 + G_i\Theta_i(\omega))$, thereby increasing the feedback gain, G_i ($i = 1, 2, 3, 4$). On the contrary, the suppression of, for instance, $\hat{\xi}$, an element of $\hat{\boldsymbol{\xi}}$, affects the other state variables, because the transformed displacement vector $\hat{\boldsymbol{\xi}}$ is not the cluster vector as was discussed before.

3.6. Implementation of cluster vector-based control

As a result of suppressing the elements of the cluster vector $\tilde{\boldsymbol{\xi}}$, the performance index for evaluating the vibration-free state of a beam decreases. The cluster vector $\tilde{\boldsymbol{\xi}}$ may be obtained by transforming the displacement vector $\boldsymbol{\xi}$ using the orthogonal matrix $\mathbf{T}_0$. Moreover, the cluster vector $\tilde{\boldsymbol{\xi}}$ may be independently controlled by the associated control force $\tilde{\mathbf{f}}$. As such, to generate a vibration-free state in the designated area of a beam, the cluster vector needs to be acquired and suppressed. Note that the transformation matrix $\mathbf{T}_0$, introduced in Eq. (85), is a function of frequency; therefore, the cluster control that generates the cluster control force vector $\tilde{\mathbf{f}}$ is also frequency dependent. Hence, the implementation of cluster control does not seem viable.

Recall that the cluster vector $\tilde{\boldsymbol{\xi}}$ and the cluster control force vector $\tilde{\mathbf{f}}$ are defined in the cluster space, whereas the implementation of cluster control is to be realized in real space. Then, the control law $\tilde{\mathbf{f}} = -\boldsymbol{\Lambda}_G\tilde{\boldsymbol{\xi}}$ (see Fig. 1) defined in the cluster space may be expressed in real space as

$$\begin{aligned} \mathbf{f} &= \mathbf{L}\mathbf{T}_0\tilde{\mathbf{f}} \\ &= -\mathbf{L}\mathbf{T}_0\boldsymbol{\Lambda}_G\tilde{\boldsymbol{\xi}} \\ &= -\mathbf{L}\mathbf{T}_0\boldsymbol{\Lambda}_G\mathbf{T}_0^{\mathrm{T}}\mathbf{L}^{\mathrm{T}}\boldsymbol{\xi}. \end{aligned} \tag{87}$$

Here, the cluster gain matrix is assumed to be described by

$$\boldsymbol{\Lambda}_G = -G\mathbf{I}, \tag{88}$$

where G and $\mathbf{I}$ are a constant feedback gain and an identity matrix, respectively. The cluster feedback gain matrix $\boldsymbol{\Lambda}_G$ in Eq. (88) is obtained by making all the feedback gains in Eq. (53) equal. This implies that each element of the cluster vector contributing to the performance index is treated evenly. The expression is still appropriate for minimizing the performance index in Eq. (86) for generating a vibration-free state. The control force vector $\mathbf{f}$ then yields

$$\begin{aligned} \mathbf{f} &= -G\mathbf{L}\mathbf{T}_0\mathbf{I}\mathbf{T}_0^{\mathrm{T}}\mathbf{L}^{\mathrm{T}}\boldsymbol{\xi} \\ &= -G\mathbf{L}\mathbf{T}_0\mathbf{T}_0^{\mathrm{T}}\mathbf{L}^{\mathrm{T}}\boldsymbol{\xi} \\ &= -G\mathbf{L}\mathbf{L}^{\mathrm{T}}\boldsymbol{\xi}. \end{aligned} \tag{89}$$

Therefore, the control law in Eq. (89) denotes that the control force $\mathbf{f}$ to be implemented in real space is no longer frequency dependent, and may then be realized by constant feedback gain in terms of the displacement vector $\boldsymbol{\xi}$. Note that performing feedback control, as expressed by Eq. (89), is tantamount to applying the control law $\tilde{\mathbf{f}} = -\boldsymbol{\Lambda}_G\tilde{\boldsymbol{\xi}}$ in the cluster space, thereby reducing the performance index without causing spillover, thus leading to the generation of a vibration-free state.

4. Radiation modes and cluster vector

A performance index for evaluating, for instance, the structural acoustic power or the potential energy (frequently used in acoustics) may be expressed in a quadratic form [16–20] with respect to the modal amplitude vector $\boldsymbol{\eta}$ as

$$J = \boldsymbol{\eta}^H \mathbf{A} \boldsymbol{\eta}, \tag{90}$$

where $\mathbf{A}$ is the error weighting matrix that is real, symmetric and positive definite. In general, the error weighting matrix $\mathbf{A}$ is not necessarily diagonal, which implies that the normal structural modes are not orthogonal contributors to the performance index. Therefore, the minimization of the modal amplitudes of the individual structural modes will not necessarily reduce the performance index. As with the minimization of the performance index, it is a common practice to describe the performance index in terms of orthogonal contributors such as radiation modes [16–20] (sometimes termed power modes [16,20]). When rewriting the performance index using the radiation mode vector $\mathbf{u} \in \mathfrak{C}^N$, which is the orthogonal contributor vector for the performance index, the modal amplitude vector $\boldsymbol{\eta}$ further expands to

$$\boldsymbol{\eta} = \mathbf{Q}\mathbf{u}, \tag{91}$$

where the unitary matrix $\mathbf{Q}$ is the orthonormal transformation matrix consisting of the eigenvectors of $\mathbf{A}$. The relationship between $\boldsymbol{\eta}$ and $\mathbf{u}$ in Eq. (91) is illustrated in Fig. 1. It is now worth connecting the performance index J, defined in Eq. (77), to the general description in Eq. (90). Substituting Eqs. (90) and (91) into Eq. (77), the performance index is then expressed as

$$\begin{aligned} J &= \hat{\boldsymbol{\xi}}^H \hat{\boldsymbol{\xi}} \\ &= \boldsymbol{\eta}^H \boldsymbol{\Phi}\mathbf{L}\mathbf{L}^{\mathrm{T}}\boldsymbol{\Phi}^{\mathrm{T}}\boldsymbol{\eta} \\ &= \mathbf{u}^H \mathbf{Q}^H \boldsymbol{\Phi}\mathbf{L}\mathbf{L}^{\mathrm{T}}\boldsymbol{\Phi}^{\mathrm{T}}\mathbf{Q}\mathbf{u}. \end{aligned} \tag{92}$$

The unitary matrix $\mathbf{Q}$ converts the matrix $\boldsymbol{\Phi}\mathbf{L}\mathbf{L}^{\mathrm{T}}\boldsymbol{\Phi}^{\mathrm{T}}$ in Eq. (92), which is symmetric and positive definite, to a diagonal matrix $\hat{\boldsymbol{\Lambda}}$. Then, the performance index will be of the form

$$J = \mathbf{u}^H \hat{\boldsymbol{\Lambda}} \mathbf{u} = \sum_{i=1}^{N} \hat{\lambda}_i u_i^2, \tag{93}$$

where

$$\mathbf{u} = \begin{pmatrix} u_1 \\ u_2 \\ \vdots \\ u_N \end{pmatrix}, \tag{94}$$

$$\hat{\boldsymbol{\Lambda}} = \mathbf{Q}^H \boldsymbol{\Phi}\mathbf{L}\mathbf{L}^{\mathrm{T}}\boldsymbol{\Phi}^{\mathrm{T}}\mathbf{Q}. \tag{95}$$

Here, the eigenvalues, $\hat{\lambda}_i$, of the matrix, $\mathbf{Q}^H \boldsymbol{\Phi}\mathbf{L}\mathbf{L}^{\mathrm{T}}\boldsymbol{\Phi}^{\mathrm{T}}\mathbf{Q}$, are apparently real and positive, and hence the terms comprising the performance index are all positive. The suppression of u_i, the elements of the radiation (power) mode vector $\mathbf{u}$, leads to the minimization of the performance index. Furthermore, the power mode eigenfunction vector $\boldsymbol{\psi}$ may be defined as

$$\boldsymbol{\psi}(x) = \mathbf{Q}^H \boldsymbol{\varphi}(x). \tag{96}$$

The above expression may be derived in the following manner:

$$\begin{aligned} \xi(x) &= \boldsymbol{\varphi}^{\mathrm{T}}(x)\boldsymbol{\eta} = \boldsymbol{\varphi}^{\mathrm{T}}(x)\mathbf{Q}\mathbf{u} \\ &= (\mathbf{Q}^H \boldsymbol{\varphi}(x))^{\mathrm{T}}\mathbf{u} \\ &= \boldsymbol{\psi}^{\mathrm{T}}(x)\mathbf{u}. \end{aligned} \tag{97}$$

It is now necessary to investigate the validity of conventional radiation (power) modes for minimizing the performance index. First, it should be noted that the radiation modes are introduced without considering the architecture of a control system; they are merely defined to describe the performance index in terms of orthogonal contributors, and hence, the consideration of sensing and actuation necessary for control is nonexistent. As stated before, if the radiation mode vector $\mathbf{u}$ is the cluster vector, the performance index expressed in terms of $\mathbf{u}$ may certainly be reduced by suppressing the respective element of the radiation mode vector. With reference to Fig. 1, the radiation mode vector may be expressed as

$$\mathbf{u} = -\boldsymbol{\psi}\mathbf{L}\mathbf{T}_0\boldsymbol{\Lambda}_G\mathbf{T}_0^{\mathrm{T}}\mathbf{L}^{\mathrm{T}}\boldsymbol{\psi}^{\mathrm{T}}\mathbf{u}. \tag{98}$$

Using the assumption for the cluster feedback gain matrix described in Eq. (88), Eq. (98) is further simplified to

$$\mathbf{u} = -G\boldsymbol{\psi}\mathbf{L}\mathbf{L}^{\mathrm{T}}\boldsymbol{\psi}^{\mathrm{T}}\mathbf{u}. \tag{99}$$

Clearly from Eq. (99), the radiation mode vector $\mathbf{u}$ is not the cluster vector, because the matrix $\boldsymbol{\psi}\mathbf{L}\mathbf{L}^{\mathrm{T}}\boldsymbol{\psi}^{\mathrm{T}}$ is not diagonal. Therefore, it is not certain whether suppressing each element of $\mathbf{u}$ will attenuate the performance index.

Consider the relationship between the cluster vector $\tilde{\boldsymbol{\xi}}$ and the radiation mode vector $\mathbf{u}$. The radiation mode vector is apparently responsible for the performance index as shown in Eq. (92), so too is the cluster vector $\tilde{\boldsymbol{\xi}}$ as in Eq. (86). The block diagram of the cluster control system shown in Fig. 1 indicates that the cluster vector is related to the radiation mode vector by the relation

$$\tilde{\boldsymbol{\xi}} = \mathbf{T}_0^{\mathrm{T}}\mathbf{L}^{\mathrm{T}}\boldsymbol{\psi}^{\mathrm{T}}\mathbf{u}. \tag{100}$$

Eq. (100) implies that the radiation mode vector $\mathbf{u}$ is transformed into $\tilde{\boldsymbol{\xi}}$ via $\mathbf{T}_0^{\mathrm{T}}\mathbf{L}^{\mathrm{T}}\boldsymbol{\psi}^{\mathrm{T}}$. When modal amplitudes u_i $(i = 1, 2, 3\ldots)$ are grouped into their respective clusters with appropriate weights, modal amplitudes then affect the reduction of the performance index as a cluster element.

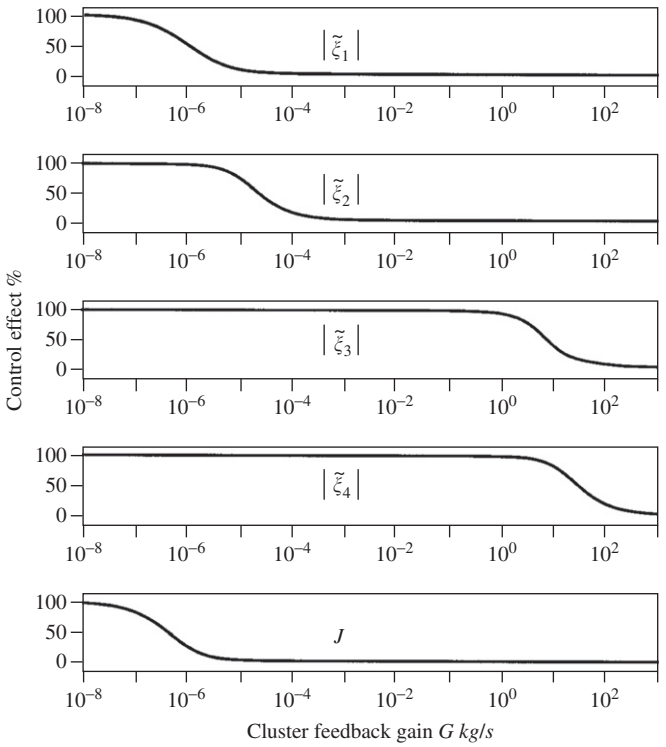

Fig. 5. Control effect for suppressing the cluster elements and the performance index versus velocity feedback gains at the 3rd structural mode.

5. Numerical simulation for generating a zone of quiet

To investigate the fundamental characteristics of the cluster control presented in this work, a numerical simulation is conducted using a clamped–clamped beam as a test vehicle, with a disturbance force of amplitude 0.05 N acting at $x_d = 1$ m. Table 1 lists beam specifications. In the numerical simulation, the control signals are fed to the four collocated control actuators, situated at $x_1 = 0.085$ m, $x_2 = 0.17$ m, $x_3 = 0.255$ m and $x_4 = 0.34$ m. The sensor placement interval is 0.085 m. These specifications are used in the experiment and will be discussed later.

As discussed in Section 2, the stability of a cluster control system is guaranteed by displacement-based feedback as well as velocity-based feedback. To investigate the attributes of cluster control, this study employs velocity feedback-based cluster control in the numerical simulation, and hence, the feedback gain G in Eq. (88) is denoted as $j\omega G$; however, the expansion in terms of the displacement-based feedback may also be undertaken in exactly the same manner.

Fig. 5 illustrates (1) control effects in terms of J and (2) the absolute cluster elements $|\tilde{\xi}_i|$ $(i = 1, 2, 3, 4)$ (expressed in percentages) at the third modal frequency (35.27 Hz) of the beam versus the cluster feedback gain G. From the figure, it is clear that as the feedback gain G increases, both the performance index J and the magnitudes of the cluster elements decrease monotonically. This allows us to understand the contribution rate of each component to the performance index; on increasing the feedback gain G, $|\tilde{\xi}_1|$ starts decreasing at $G = 10^{-7}$ kg/s, while the other three elements remain constant. Then, $|\tilde{\xi}_2|$ follows at $G = 10^{-5}$ kg/s. Observe that the curve of the performance index is quite similar to that of $|\tilde{\xi}_1|$, implying that the cluster element $\tilde{\xi}_1$ is the greatest contributor to the control effect expressed by J.

Fig. 6 shows the control effects in terms of $\hat{J}$, and the estimated dominant state variables of the beam, $\hat{\xi}$, $\hat{\theta}$, $\hat{m}_x$ and $\hat{q}_x$. In contrast to the control effect demonstrated in Fig. 5, all of the estimated state variables

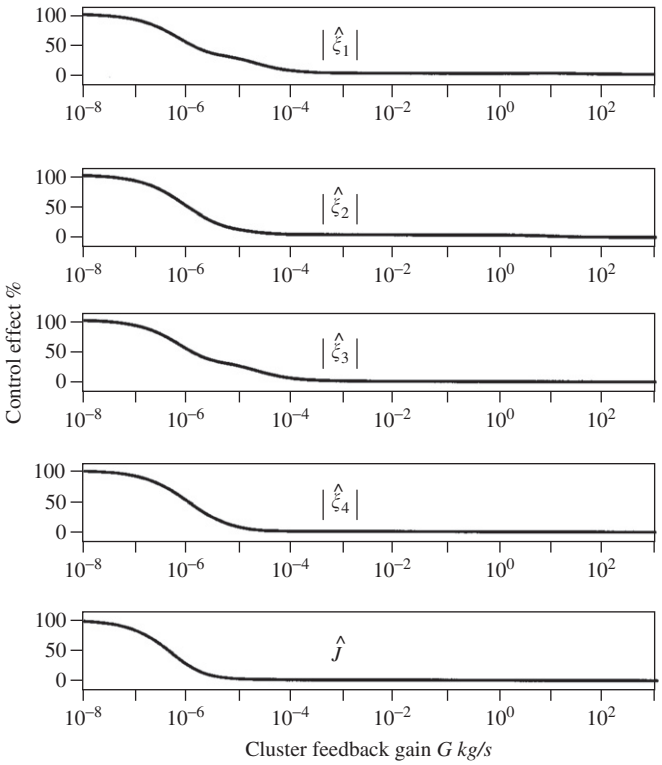

Fig. 6. Control effect for suppressing the estimated state variables and the performance index versus velocity feedback gains at the 3rd structural mode.

begin to decrease almost simultaneously at $G = 10^{-7}$ kg/s, implying that the contribution rate of each estimated state variable to the control effect for generating a vibration-free state is comparable. Observe that the curve of J in Fig. 5 and that of $\hat{J}$ in Fig. 6 are the same as proved in Eq. (86). The suppression of the cluster elements and the four estimated state variables reduces the control effect for generating a vibration-free state in the designated region of a beam. Note that the control effectiveness increases in proportion to the cluster feedback gain, as expressed in Eq. (84); an increase of G leads to a decrease in the gain of the respective transfer function connecting a cluster element and the corresponding disturbance force.

Fig. 7 depicts the time histories of the four state variables of the beam after the application of cluster control driven with a velocity feedback gain of 100 kg/s. Comparison of Figs. 4 and 7 allows one to comprehend the nature of the vibration-free state of a beam; two nodes appear in the displacement time histories when the amplitudes of the slope and the shear force at the nodes are at a maximum, as shown in Fig. 4. Thus, only two of the four state variables at the so-called node are zero, and hence they are not vibration-free. In contrast, after cluster control, the magnitudes of the four state variables, which uniquely resolve the dynamic behavior

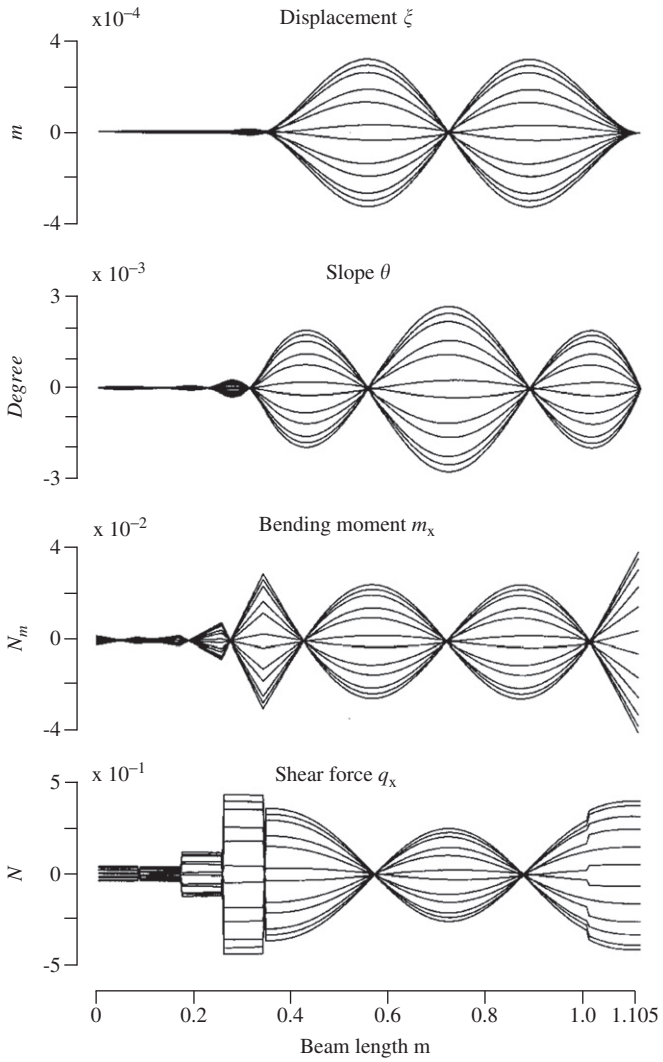

Fig. 7. Time histories of four state variables of a clamped–clamped beam after cluster control with a velocity-based feedback gain of $G = 100$ kg/s at the 3rd structural mode.

of a beam, are significantly reduced, as shown in Fig. 7. The maximum displacement value in the region is reduced to only 0.17% of that before control. The magnitudes of all the four dominant variables in the region are not completely nullified, because the control effect is dependent on the cluster feedback gain; on further increasing the cluster feedback gain, the values of all the four variables continue to decrease, resulting in a vibration-free state of a beam.

The time histories of the displacement response of the clamped–clamped beam at 25 Hz with the cluster feedback gain varying from 1 to 50 kg/s are shown in Fig. 8. In the region where cluster control is performed, the amplitude of the displacement is reduced as the cluster feedback gain increases.

Fig. 9 illustrates the frequency response of the beam displacement at $x_2 = 0.17$ m (the second sensor/actuator location from the left) for a frequency range up to 100 Hz. As the cluster feedback gain G increases, the displacement response decreases throughout the whole frequency range of interest. Note that the control effect pattern of the frequency response is significantly different from that of the conventional vibration control strategy. Not only does cluster feedback augment structural damping, but the asymptote of the displacement response also moves downwards as the cluster feedback gain increases.

Resonance peaks appear at 13, 35 and 70 Hz in the frequency range of interest due to cluster control, and hence, grave concerns may arise if the peaks lead to the instability of a feedback control system. However, the stability of the cluster feedback control system was already proved to be unconditionally stable in Section 2. Therefore, it is not clear whether the peaks are due to the effect of control stability or not. To decipher this phenomenon, we take a look at the time histories of the four state variables shown in Fig. 7. The final goal of cluster control is to generate a vibration-free node at the designated location; however, the control effect is gain-dependent, and hence the process shown in Fig. 7 ($G = 100$ kg/s) to arrive at the final goal. We focus on the left side of the four state variables for the region between the fourth sensor/actuator location from the left ($x_4 = 0.34$ m) and the right end of the beam, which is clamped. The figure shows that the beam in this region, which is out of the control target, may be approximately considered a clamped–clamped beam of length 0.765 m (= 1.105–0.34 m). The modal frequencies of such a beam are close enough to the three above-mentioned frequencies. Hence, the resonance peaks appearing in Fig. 9 do not lead to the instability of the feedback control system.

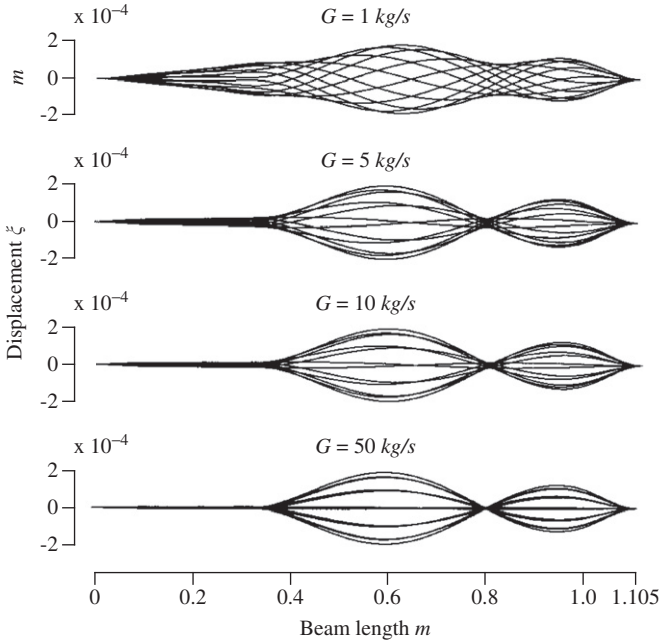

Fig. 8. Time histories of displacement response after velocity-based cluster control by varying feedback gain from 1 to 50 kg/s.

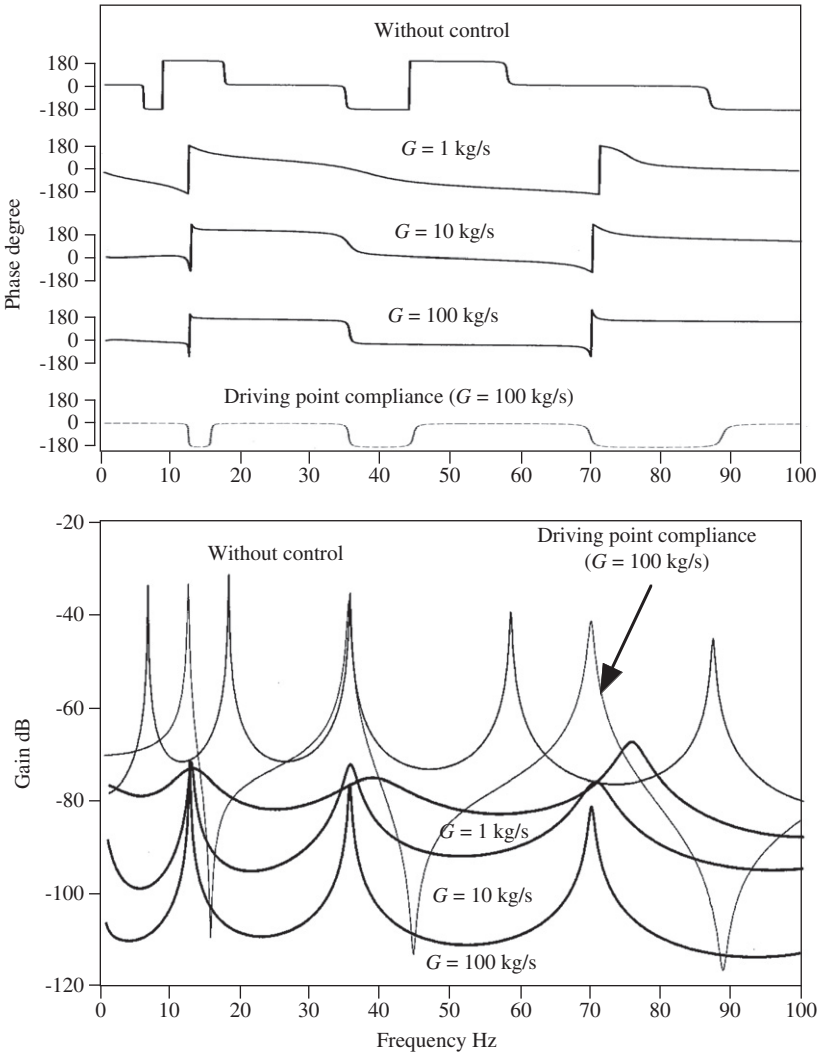

Fig. 9. Frequency characteristics of the displacement response of a clamped–clamped beam before and after cluster feedback with the feedback gain varying from 1 to 100 kg/s.

6. Experiment

Fig. 10 shows the test rig for the cluster control system; the specifications of the beam used in the experiment are the same as those used in the numerical analysis (see Table 1). An envelope of the beam displacement distribution was obtained using a wave visualization system that had been developed for this experiment. The wave visualization system consists of a gap sensor array positioned along the beam at 8.5 cm intervals. The sensor outputs, simultaneously acquired by a data logger, were directly transferred to the wave visualization system to draw the envelopes of the displacement response of the beam. Four electro-dynamic actuators (for cluster actuation) and four acceleration sensors (for cluster filtering) are attached at the same beam positions used in the simulation, i.e., $x_1 = 0.085$ m, $x_2 = 0.17$ m, $x_3 = 0.255$ m and $x_4 = 0.34$ m. In addition, a piezo-ceramic actuator is attached at $x_d = 1$ m for exciting the beam.

Fig. 11(a) depicts the experimental results of the time histories of the displacement response of the target beam, driven at the second modal frequency, 14.2 Hz, prior to cluster control. The maximum displacement amplitude is approximately 2.2 mm. Fig. 11(b) illustrates the time histories of the displacement response after

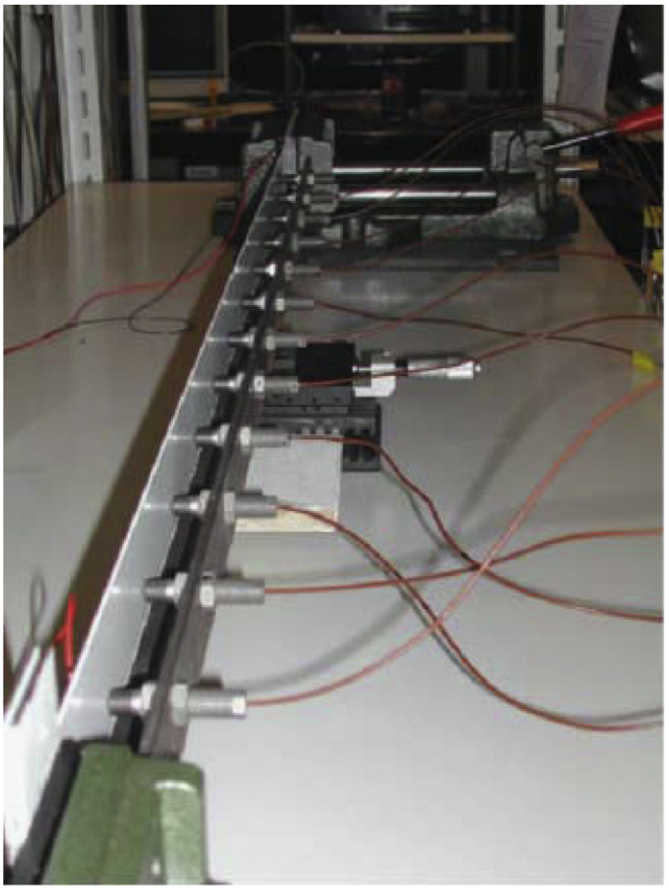

Fig. 10. Test rig of cluster control.

cluster control. As seen from the figure, the maximum value of the displacement is reduced to 70 μm, i.e., about 3.2% of that before control. Note that the vibration-free state is generated in the designated region of the beam, wherein sensors and actuators are placed. The displacement value in this region, for instance at $x_2 = 0.17$ m, is 9.5 μm, which is about 0.4% of the maximum displacement response value before control. Fig. 11(c) shows the time histories of the displacement response for the beam excited at the third modal frequency (28.5 Hz) before cluster control. The maximum displacement response amplitude is 8.4 mm, which is reduced to 40 μm after control, i.e. 0.48% of the value before control, as shown in Fig. 11(d). In the 'zone of quiet', the displacement amplitude is reduced to 8 μm at $x_2 = 0.17$ m, i.e. 0.1% of the maximum displacement before control. It is found that the experimental results are not as good as those predicted by the simulations because a sufficient feedback gain was not provided. This is due to the following reasons: (1) the signal/noise ratio for signal processing was not high; (2) the amplifiers saturated when feedback gain was increased; (3) the control power of the electro-dynamic actuators was not sufficient; (4) sensor resolution was not very fine, due to the integration of acceleration output using an analog integrator; and (5) the phase properties were affected by a high-pass filter used to avoid signal drift.

Fig. 12 depicts the dynamic mobility of the beam, before and after cluster control, measured at the second sensor location from the left ($x_2 = 0.17$ m), the beam being provided with random excitation at $x_d = 1$ m. Because of the load effect due to the accelerometer pickups attached on the beam, the resonance frequencies slightly reduced compared to those in the analysis. In the experiment, cluster feedback gain was determined in situ while monitoring the waveforms of the beam response being suppressed. To drive the actuators, a feedback gain of 0.37 A/V was applied between the charge amplifier and the power amplifier outputs. Observe that the asymptote of the frequency response shifted down by 10 dB throughout the frequency range of

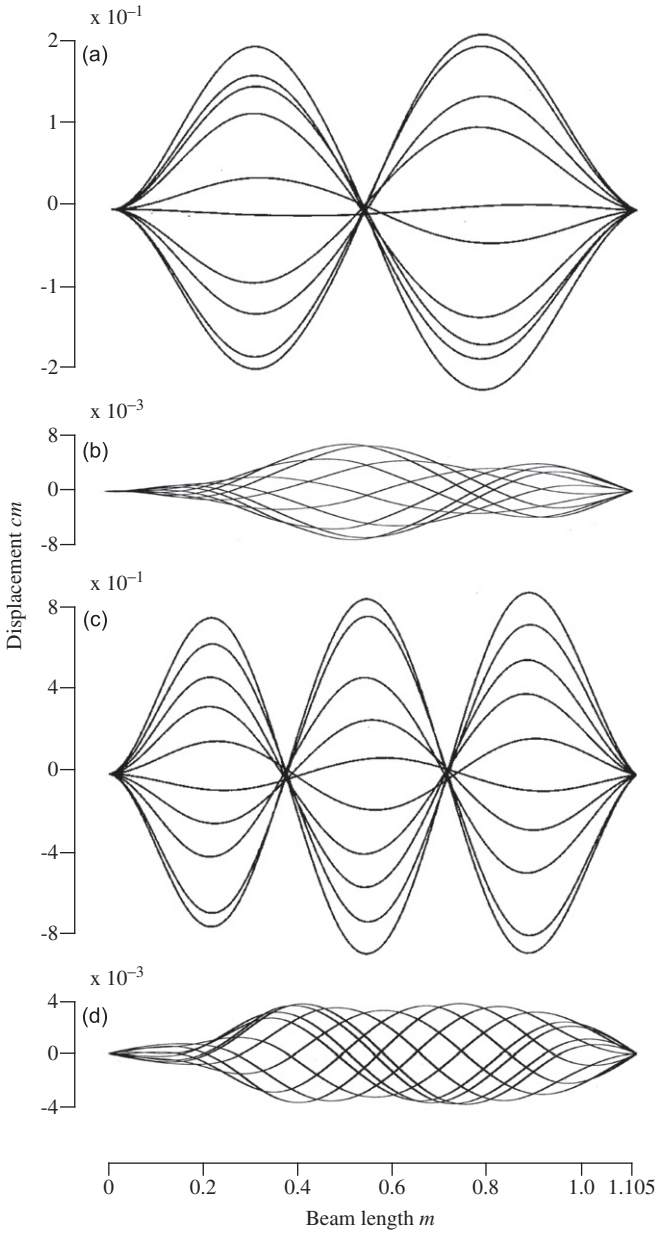

Fig. 11. Experimental results of the time histories of a displacement response of a clamped–clamped beam (a), (b) before and after active cluster control at the second and (c), (d) the third modal frequencies.

interest, which is characteristic of cluster control. For instance, the control effect at the third modal frequency was 36 dB, about 1.6% of that without control. Because of the high-pass filter, which has a cut-off frequency of 0.1 Hz to avoid signal drift, the frequency response at low frequencies is toothed, thereby imposing restrictions on feedback gain increments.

7. Conclusions

With the aim of generating a vibration-free state in the designated area of a target beam, active cluster control was presented. Active cluster control consists of both cluster filtering and cluster actuation.

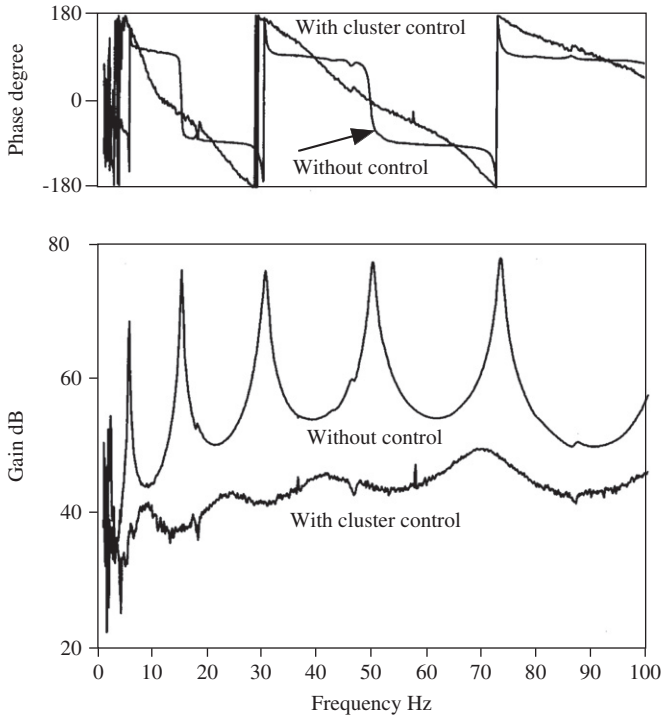

Fig. 12. Dynamic mobility of a clamped–clamped beam before and after cluster control.

Cluster filtering extracts the state variables of a beam, which governs the dynamic behavior of a beam, and cluster actuation suppresses the extracted state variables without causing spillover. It was mathematically verified that cluster control guarantees the unconditional stability of the control system. It was found that four state variables of a beam must be extracted and suppressed to generate a vibration-free state in the designated area of a beam. For this purpose, a cluster vector, which is a common link between cluster filtering and cluster actuation, was introduced. It was also found that the suppression of a performance index, expressed in terms of the cluster vector, generates a vibration-free state in the beam, whereas the suppression of conventional orthogonal contributors, such as radiation modes, does not. Moreover, numerical simulation showed that active cluster control can generate a vibration-free state in the designated region of a target beam. Numerical simulation was followed by experiment, verifying the validity of cluster control, as presented in this work.

Acknowledgments

The support for this work from the Japan Society for the Promotion of Science and Tokyo Metropolitan University is gratefully acknowledged.

References

[1] M.J. Balas, Active control of flexible systems, *Journal of Optimization Theory and Applications* 25 (1978) 415–436.
[2] M.J. Balas, Direct velocity feedback control of large space structure, *Journal of Guidance* 2–3 (1979) 252–253.
[3] J.N. Aubrun, Theory of the control of structures by low-authority control, *Journal of Guidance and Control* 3 (1980) 444–451.
[4] D.R. Vaughan, Application of distributed parameter concepts to dynamic analysis and control of bending vibrations, *ASME Journal of Basic Engineering* (1968) 157–166.
[5] A.H. von Flotow, J.B. Schafer, Wave absorbing controllers for a flexible beam, *Journal of Guidance* 9 (1986) 673–680.
[6] G.M. Procopio, J.E. Hubbard Jr., Active damping of a Bernoulli–Euler beam via end point impedance control using distributed parameter techniques, *ASME Design Technology Conference* (1987) 35–46.
[7] B.R. Mace, Active control of flexural vibrations, *Journal of Sound and Vibration* 114 (1987) 253–270.

[8] D.W. Miller, S.R. Hall, A.H. von Flotow, Optimal control power flow at structural junctions, *Journal of Sound and Vibration* 140 (1990) 475–497.
[9] D.G. MacMartin, S.R. Hall, Control of uncertain structures using an H-infinity power flow approach, *Journal of Guidance* 14 (1990) 521–530.
[10] N. Tanaka, Y. Kikushima, Active wave control of a flexible beam (proposition of the active sink method), *JSME International Journal* 34 (1991) 159–167.
[11] N. Tanaka, Y. Kikushima, Active wave control of a flexible beam (fundamental characteristics of an active sink system and its verification), *JSME International Journal* 35 (1992) 236–244.
[12] N. Tanaka, Y. Kikushima, Optimal vibration feedback control of an Euler–Bernoulli beam: toward realization of the active sink method, *ASME Journal of Vibration and Acoustics* 121 (1999) 174–182.
[13] N. Tanaka, S.D. Snyder, Cluster control of a distributed-parameter planar structure MAC (middle authority control), *Journal of the Acoustical Society of America* 112 (2002) 2798–2807.
[14] N. Tanaka, R. Fukuda, C.H. Hansen, Acoustic cluster control of noise radiated from a planar structure, *Journal of the Acoustical Society of America* 117 (2005) 3686–3694.
[15] N. Tanaka, K. Kobayashi, Cluster control of acoustic potential energy in a structural/acoustic cavity, *Journal of the Acoustical Society of America* 119 (2006) 2758–2771.
[16] S.D. Snyder, N. Tanaka, On feedforward active control of sound and vibration using error signals, *Journal of the Acoustical Society of America* 96 (1993) 2302–2312.
[17] S.J. Elliot, M.E. Johnson, Radiation modes and the active control of sound power, *Journal of the Acoustical Society of America* 94 (1993) 2194–2204.
[18] K.A. Cunefare, M.N. Currey, On the exterior acoustic radiation modes of structures, *Journal of the Acoustical Society of America* 96 (1994) 2303–2312.
[19] M.N. Currey, K.A. Cunefare, The radiation modes of baffled finite plates, *Journal of the Acoustical Society of America* 98 (1995) 1570–1580.
[20] N. Tanaka, S.D. Snyder, C.H. Hansen, Distributed parameter modal filtering using smart sensors, *ASME Journal of Vibration and Acoustics* 118 (1996) 630–640.